Published in J. Phys. Chem. C 2007, 111, 5416

Infrared Spectroscopic Study of the Adsorption of HCN by γ-Al_2O_3: Competition with Triethylenediamine for Adsorption Sites

Sunhee Kim[≠], Dan C. Sorescu[#], and John T. Yates, Jr.*[≠]

[≠]Surface Science Center, Department of Chemistry,

University of Pittsburgh, Pittsburgh PA 15260

[#]U.S. Department of Energy, National Energy Technology

Laboratory, Pittsburgh, PA 15236

Abstract

The adsorption and vibrational properties of chemisorbed HCN on Lewis acid sites, Lewis base sites, and Brønsted Al-OH acid sites on a partially hydroxylated γ-Al_2O_3 surface have been obtained by a combination of FTIR and density functional theory studies. The vibrational modes from the molecular and dissociative adsorption of HCN were assigned by using deuterium and ^{13}C labeled $D^{13}CN$ molecules at 170 K. In addition, η^2(C, N)-HCN bonding is also found from the ν(C=N) vibrational spectra. Good correlation of the calculated vibrational frequencies for the adsorbed species with experimental data is found.

The effect of triethylenediamine (TEDA) (also called 1, 4-diazabicyclo [2.2.2]octane, DABCO) on the adsorption of hydrogen cyanide (HCN), on the high area γ-Al_2O_3 surface has been investigated using transmission FTIR spectroscopy. During HCN adsorption on TEDA-functionalized surfaces there is no spectral change or emerging feature in either the TEDA or HCN spectral regions, indicating that no direct interaction occurs between these two molecules. Instead, we found that TEDA competes with HCN for the active sites on γ-Al_2O_3. The observed ν(C≡N) mode on a TEDA-precovered surface is due to the HCN adsorption on Lewis base sites (Al-***O***-Al) which are less affected by TEDA pre-adsorption.

Introduction

Research on the adsorption of HCN on oxide surfaces has a long history,[1-5] but the precise identification of different binding modes based on infrared spectroscopic measurements is still lacking, especially on the γ-Al_2O_3 surface. It is generally accepted

that HCN adsorbs molecularly as well as dissociatively on oxide surfaces, and polymerization of HCN is also reported. On silicate and titania surfaces, the formation of isocyanide species (M-NC) as well as cyanide species (M-CN) from HCN adsorption has been observed and assigned by using isotopically-labeled hydrogen cyanide.[2,4] In contrast to the dissociative adsorption of HCN, studies of the non-dissociated species and their binding sites have not been made, so that the vibrational assignment of HCN on Lewis acid, Lewis base, and Brønsted acid sites has not been made. This investigation focuses on this point. In addition, we have observed η^2 (C,N)-HCN binding to γ-Al_2O_3 where N and C atoms bond simultaneously to a pair of Al and O sites at 170 K. The experimental results are compared to DFT calculations.

We have also investigated the role of triethylenediamine (TEDA) (also called 1, 4-diazabicyclo[2.2.2]octane, DABCO) functionalization of γ-Al_2O_3 on the adsorption of hydrogen cyanide. The TEDA molecule is used as an impregnant to enhance the adsorption of chemical agents and other toxic industrial compounds such as HCN, ClCN, SO_2, H_2S, CH_3I, etc. on activated charcoal adsorbents.[6-9] It is believed that the amine groups present on the opposite ends of the TEDA molecule provide the chemical bonding to the charcoal surface as well as an amine site on the opposite end of the TEDA molecule for subsequently adsorbed species. In order to enhance the sorptive properties of TEDA-treated charcoal, additional functionalization with Cu^{2+} cations is often employed. For HCN adsorption, Cu^{2+} functionalization of TEDA-treated surfaces has been shown to be important.[10] Theoretical studies suggest the existence of significant interactions between the Cu^{2+} center and HCN with binding energies for the HCN···Cu^{2+}

complex as high as ~ 112 kcal mol^{-1}, whereas the HCN···TEDA complex exhibits a much smaller binding energy of only ~ 7 kcal mol^{-1}.[11]

In this work, no evidence of a direct interaction between TEDA and HCN molecules is found. Instead, it is shown that TEDA competes with HCN for the active sites on γ-Al_2O_3. The saturated coverage of adsorbed HCN molecules on TEDA-precovered γ-Al_2O_3, judging from the integrated absorbance of the ν(C≡N) modes, falls to ~ 1/7 of its value on unfunctionalized γ-Al_2O_3.

II. Experimental and Computational Methods

A. Experimental. The experimental methods used in this work were described in detail previously.[12] The high vacuum infrared cell system (base pressure ≅ 1 × 10^{-8} Torr) was designed to provide temperature control of a high area solid adsorbent from 83 K to above 1400 K. The cell has two KBr windows, allowing the IR beam to pass through a tungsten grid, into which γ-aluminum oxide powder is pressed.[13,14]

The Al_2O_3 powder was obtained from Guild Associates (surface area = 250 m^2/g). The Al_2O_3 sample was briefly heated to 1000 K in vacuum to produce a highly dehydroxylated surface.[13-16] The triethylenediamine (TEDA) and triethylenemonoamine (TEMA also called 1-azabicyclo[2,2,2]octane, ABCO) were obtained from Aldrich. HCN was prepared by the reaction of KCN with H_2SO_4.[17] $D^{13}CN$ was obtained commercially. The isotopic purity of the $D^{13}CN$ was checked using a quadrupole mass spectrometer (QMS) and by IR spectroscopy and was found to be higher than 90 % (the main impurity is $H^{13}CN$).

TEDA vapor was admitted into the chamber, with the temperature of the alumina sample at 300 K, to form the adsorbed phase of TEDA.[12] After TEDA adsorption, the chamber was evacuated by a turbo-molecular pump and then the TEDA-functionalized alumina sample was exposed to HCN(g) at 170 K. The infrared spectra were recorded at each indicated temperature with a Bruker TENSOR 27 FT-IR spectrometer. Each spectrum was obtained by averaging 64 interferograms with 2 cm^{-1} resolution and the background spectrum, taken through the empty grid region, was subtracted.

B. Computational Method. The theoretical work performed in this study focused on a description of the chemisorption and vibrational properties of HCN and CN species adsorbed on the γ-Al_2O_3 surface. The computational method used for this purpose is similar to that employed by us to describe the chemisorption properties of TEDA and CO molecules on the same surface.[18] As a result, here we will provide only the essential elements for the current work.

The calculations were performed using the Vienna *ab initio* simulation package (VASP).[18-21] This program evaluates the total energy of periodically repeating geometries based on density-functional theory and the pseudopotential approximation. In this case the electron-ion interaction has been described by fully non-local optimized ultrasoft pseudopotentials (USPPs) similar to those introduced by Vanderbilt.[22,23] Periodic boundary conditions are used, with the one-electron pseudo-orbitals expanded over a plane-wave basis set with a cutoff energy of 495 eV.

The adsorption properties of HCN and CN species on the γ-Al_2O_3 surface have been done using PW91 generalized gradient approximation (GGA) of Perdew *et al.*[24] Spin polarized calculations have been considered for the case of radical species. The

sampling of the Brillouin zone was performed using a Monkhorst-Pack scheme[25] using a grid mesh with a k-point separation of 0.05 $Å^{-1}$.

The crystallographic structure of bulk γ-alumina was taken according to the structure reported in Ref. 26. We have considered the adsorption properties on both (100) and (110) surfaces of γ-Al_2O_3, as these surface orientations have been shown to be predominant for the exposed surface.[26-28] These surfaces have been simulated using slab models with at least eight atomic planes. Each slab was taken to be symmetrical to avoid unphysical dipole-dipole interactions between neighbor slabs. Further details of the relaxation and surface energies for these surfaces can be found in our previous work.[18] We note here the diversity of surface sites on these surfaces. Specifically, the (100) surface presents five-fold coordinated aluminum atoms (denoted as Al_V) and three-fold coordinated oxygen atoms (denoted as μ_3-O) while the (110) surface presents several types of coordinated Al and O atoms, namely three-fold Al_{III} (I) and four-fold Al_{IV} (II and III) aluminum sites and two-fold (μ_2-O) and three-fold (μ_3-O) oxygen atoms.

Beside an accurate description of the γ-Al_2O_3 surface as described in our previous work[18] the current plane-wave DFT method employed is also adequate for description of the geometric parameters and vibrational properties of HCN and CN species. For the HCN(g) molecule, the optimized bond lengths were found equal to r(C-N) = 1.156 Å, r(C-H) = 1.069 Å while for the CN(g) radical the equilibrium distance is 1.065 Å. These values are in very good agreement to corresponding experimental values of r_{exp}(C-N) = 1.153 Å, r_{exp}(C-H) = 1.065 Å for HCN, and of 1.172 Å for the CN radical. Similarly, the calculated vibrational frequencies for the HCN molecule of ν(C-N) = 2107 cm^{-1}, ν(C-H) = 3382 cm^{-1}, and for CN radical of 2067 cm^{-1} were found to reproduce sufficiently

accurately the experimental data, namely ν_{exp}(C-N) = 2097 cm^{-1}, ν_{exp}(C-H) = 3311 cm^{-1} for the HCN molecule, and 2068 cm^{-1} for the CN radical.

On the Based on this comparison to experimental data, it is expected that the current computational method, previously proven to be accurate for the description of the adsorption properties of TEDA and CO molecules on γ-Al_2O_3,[18] is also adequate to describe the chemisorption properties of HCN and CN species on γ- Al_2O_3 surfaces.

III. Results: Experimental Studies

A. HCN Adsorption on Clean γ-Al_2O_3 Surfaces. Figures 1 and 2 show the IR spectra for the HCN adsorption at 170 K, followed by heating up to 290 K at an HCN equilibrium pressure of ~15 mTorr. The infrared spectra in the ν(O-H), ν(C-H) region and the ν(C≡N) region are shown and group frequency assignments for the various species are indicated in bold letters on the labels in the spectra. In addition, for ease of understanding, the bold arrows indicate the growth or loss of absorbance upon heating. Two broad bands develop in the 3600 cm^{-1} – 3300 cm^{-1} region, and in the 3300 cm^{-1} – 2800 cm^{-1} region, and a sharp peak at ~ 3300 cm^{-1} is observed to develop upon HCN exposure at 170 K as shown in Figure 1. The HCN molecule can adsorb on the surface either via a nitrogen atom or via a hydrogen atom. The hydrogen bonding of HCN molecules through the N atom to Al-O**H** groups (Brønsted acid sites) produces the associated OH species (3600 cm^{-1} – 3300 cm^{-1}), consuming the higher frequency isolated Al-OH species, as is often observed for hydrogen bonding of adsorbed molecules (stages of adsorption not shown). In addition to this type of surface binding, the HCN adsorption on $\mathbf{Al^{3+}}$ ions (Lewis acid sites) occurs via the nitrogen atom of HCN. Both of these HCN

bonding structures produce a sharp ν(C-H) mode for HCN as observed at ~ 3300 cm^{-1}. In addition to Brønsted acid and Lewis acid sites, Lewis base sites also exist on partially dehydroxylated γ-Al_2O_3 (hereafter denoted Al-***O***-Al). HCN molecules bind to these sites via hydrogen bonding, producing strongly red-shifted and broadened C-H modes as seen in the ~ 3300 cm^{-1} – ~ 2800 cm^{-1} spectral region. As the Al-OH···NCH and the Al-O···HCN species are depopulated by heating to 290 K, the ν(C-H) mode at ~ 3300 cm^{-1} decreases only slightly in absorbance, indicating that Al^{3+}···NCH species remain on the surface up to 290 K.

The spectra in the ν(C≡N) vibrational region are shown in Figure 2 for heating in the range 170 K – 290 K. Because of the diversity of the HCN binding structures, at least four overlapping ν(C≡N) absorption bands appear at 170 K. Upon heating in the temperature interval 170 K – 290 K, two ν(C≡N) features intensify at ~ 2179 cm^{-1}(weak) and at ~ 2100 cm^{-1} (strong). During heating the other ν(C≡N) modes at ~ 2147 cm^{-1} and ~ 2079 cm^{-1} decrease at different rates. At 290 K, the mode at ~ 2147 cm^{-1} is still visible while the mode at 2079 cm^{-1} is no longer visible. The prominent growth of intensity of the ~ 2100 cm^{-1} mode upon heating is attributed to HCN decomposition on the surface, producing Al-NC species.

In the same manner the spectra of the adsorbed $D^{13}CN$ on γ-Al_2O_3 are shown in Figure 3 and 4. Spectral features due to Al-OH species hydrogen bonded to $N\equiv{}^{13}CD$ are observed, as in Figure 1, but are not shown here. The observation of the formation of isolated Al-OD modes[15,29] from $D^{13}CN$ adsorption indicates that the ^{13}C-D bond breaks upon adsorption, leading to ^{13}CN species formation (as will be shown in Figure 4). In addition various ν(^{13}C-D) modes are observed to form which are analogous to the ν(C-H)

modes shown and assigned in Figure 1. The higher relative intensity of the broad band in the 2600 cm^{-1} – 2300 cm^{-1} region is due to associated Al-OD species whose absorbance underlies the $\nu(^{13}C\text{-}D)$ region. The analogous associated Al-OH modes do not overlap the ν(C-H) modes in Figure 1. In addition a broadening of the shoulder is observed in the $\nu(^{13}C{\equiv}N)$ region (< 1900 cm^{-1}), indicating the additional $D^{13}CN$ species bound to Al-OD groups (as will be shown in Figure 4).

By using double labeling in $D^{13}CN$ we are able to separate ν(C≡N) modes for $D^{13}CN$ surface species and for ^{13}CN surface species. The mode for non-dissociated $D^{13}CN$ species will be lower in frequency than the modes for chemisorbed ^{13}CN species. This allows us to separate the overlapping of HCN- and CN- derived modes which are present in Figure 2. As shown in Figure 4, these two types of species are separated spectroscopically. Upon heating from 170 K to 290 K, Al-N≡^{13}C and Al-^{13}C≡N species are observed to develop together as $D^{13}CN$ thermally dissociates. The various surface species derived from undissociated $D^{13}CN$ are displayed at lower frequencies. It may be seen from comparing data in Figures 4 with 2 that the thermal decomposition of the hydrogen cyanide molecule is clearly witnessed without spectral overlap in the wavenumber region below ~ 1975 cm^{-1}. A comparison of the frequencies and isotopic shifts for HCN- and DCN-derived surface species is given in Table I, along with comparisons to the literature.

Figure 5 shows the IR spectra for the HCN adsorption at 170 K in the ν(C=N) vibrational region upon increasing the equilibrium pressure of HCN. In addition to the various ν(C≡N) modes in Figure 2, a spectral feature is observed at ~ 1698 cm^{-1} upon HCN exposure indicating η^2(C, N)-HCN bonding on γ-Al_2O_3. The η^2(C, N)-HCN and

Al^{3+}···NCH species are depopulated by heating to 400 K, and the dissociatively adsorbed species (Al-CN and Al-NC) still remain on γ-Al_2O_3 (not shown here).

In summary, for HCN adsorption on γ-Al_2O_3, we find that HCN binds to Al-OH groups and to Al-***O***-Al Lewis base centers, as well as to Al^{3+} centers. Thermal dissociation occurs in the range 170 K – 290 K producing Al^{3+}-NC and Al^{3+}-CN species, and deuterium ions generated from D-^{13}CN(a) decomposition react (or exchange with Al-OH groups) to produce Al-OD groups. In addition η^2(C, N)-CN bonding occurs as evidenced by the ~ 1698 cm^{-1} mode in the C=N double bond vibrational region.

B. HCN Adsorption on TEDA-precovered γ-Al_2O_3 Surfaces. In Figure 6, HCN was adsorbed on top of a TEDA-functionalized γ-Al_2O_3 surface. Spectra in the ν(C≡N) region are chosen for display. The dashed spectrum shows the spectrum for HCN adsorption on to pure γ-Al_2O_3 at 170 K (reproduced from Figure 2) and includes two or more bonding structures of HCN. The comparison shows that TEDA effectively competes for various HCN adsorption sites causing the integrated ν(C≡N) spectra to be reduced to 1/7th the value obtained in the absence of pre-adsorbed TEDA. Upon heating above 170 K the growth of Al-NC species (~ 2100 cm^{-1}) is also observed (not shown), just as seen for the clean γ-Al_2O_3 (in Figure 2). The loss of Al_2O···HC≡N and Al^{3+}···N≡CH species accompanies the HCN dissociation at T > 170 K (not shown).

Figure 7 displays a comparison of HCN adsorption on TEDA and TEMA-precovered γ-Al_2O_3 surfaces. The purpose of our study of TEMA is to remove the outer N atoms of the amine functionalized surface to check for any influence of the outer N functionality on HCN adsorption. The two spectra of Figure 7 show that no significant ν(C≡N) spectral differences are seen for HCN adsorption on TEDA and TEMA-

functionalized γ-Al_2O_3 surfaces. The TEMA coverage is slightly higher than the TEDA coverage in this comparison. Thus the outer amine group is not involved in bonding HCN to TEDA-functionalized γ-Al_2O_3 and ***only site blocking effects by TEDA and TEMA are observed***.

Another spectroscopic evaluation of the interaction of TEDA and HCN can be made by carefully looking for changes in the IR spectra of TEDA during adsorption of HCN. This is seen in Figure 8, where two spectral regions, ν(C-H) and δ(C-N) for TEDA, are shown as the coverage of HCN is increased at 170 K. No spectral shift in the TEDA vibrational modes is observed for both frequency regions. Shifts, particularly in the δ(C-N) mode, have previously been shown to occur upon chemical interaction with the nitrogen atoms of TEDA molecules.[12] These results, coupled with others shown above, indicate that adsorbed TEDA molecules on γ-Al_2O_3 do not undergo chemical interactions with adsorbed HCN species.

IV. Results: Theoretical Studies

A. HCN and CN Adsorption on (100) and (110) Surfaces of γ-Al_2O_3. The adsorption properties of HCN molecules on the γ-Al_2O_3 surface were investigated for the case of (100) and (110) surface orientations using the slab models described in Section II B. The corresponding adsorption energies calculated throughout this work were obtained based on the expression

$$E_{ads} = E_{molec} + E_{slab} - E_{(molec+slab)} \quad (1)$$

where E_{molec} is the energy of the isolated adsorbate molecule in its equilibrium position, E_{slab} is the total energy of the slab and $E_{(molec+slab)}$ is the total energy of the adsorbate/slab

system. The only exception from the above definition was considered in the case when HCN adsorption is mediated by OH groups. In this case E_{slab} energy was taken as the total energy for the slab with the adsorbed OH group. A positive E_{ads} as determined based on Eq. (1) corresponds to a stable adsorbate/slab system. The energy of the isolated adsorbate molecule was determined from calculations performed on a single molecule in a cubic cell of length 12 Å. The same Brillouin-zone sampling has been used to calculate the energies of the bare slab and of the molecule-slab systems. The corresponding results corresponding to adsorption of HCN on (100) and (110) surfaces are given in Table 2 while representative configurations are depicted in Figures 9 (a)-(g).

As can be seen from data presented in Figure 9 and Table 2 several bonding types of HCN molecule to the surface can take place. The main bonding mechanism is seen for the case of HCN adsorption at unsaturated Al sites with the N end of the molecule oriented toward the surface. On the (100) surface the calculated binding energies were found to range between 7.4 – 12.7 kcal/mol while on the (110) surface the binding energies increase up to 27.5 kcal/mol. The corresponding Al…N separations range between 2.166-1.985 Å. The largest adsorption energy is seen in the case of (110) surface when the molecule adsorbs at the highly unsaturated Al_{III}(I) site (see Figure 9 (d)) on the (110) surface. On the (100) surface the calculated C-N vibrational frequencies of the HCN molecule range from 2155 – 2169 cm^{-1} while on the (110) surface the corresponding vibrational frequencies are blue shifted in the range 2166 – 2201 cm^{-1} consistent to the larger binding energies observed on this surface.

A second set of HCN adsorption configurations identified correspond to η^2(C, N)-HCN species where both C and N atoms are simultaneously bonded to a pair of nearby Al

and O surface sites. Such bonding configurations are possible on both (100) and (110) surfaces but only those on the later surface were found to be stable with respect to the energy of the isolated HCN molecule and of the slab surface. As a result, in Table 2 we provide only the data corresponding to η^2(C, N)-HCN configurations on the (110) surface (see also Figures 9(e)). For these configurations we found that the corresponding C-N bonds are elongated on average by 0.1 Å relative to the standing up states indicating a softening of these bonds. Consistent to these changes the corresponding C-N vibrational frequencies are red shifted into the range 1634 – 1710 cm^{-1}.

The third category of bonding configurations of HCN molecules, denoted O··HCN in Table 2, correspond to hydrogen bonding to surface O atoms through the H end of the molecule (see also Figures 9(b),9(f)). In these cases the binding energies were found to be smaller than in previous cases with values in the range 2.2 – 5.3 kcal/mol. Additionally, only small shifts relative to the gas phase values of C-N vibrational modes are seen with values in the range 2084 – 2094 cm^{-1}.

Finally, we have analyzed the possibility of HCN molecules adsorbing at Al-OH Brønsted acid sites (see configurations in Figure 9(c), 9(g)) and data in Table 2(d). Our calculations in this case were restricted to the case of small coverages of OH species as this is expected to be the case for a surface annealed up to 1000 K in high vacuum conditions as was done in the current study. We found that the HCN molecule can adsorb on hydroxyl groups by formation of O-H···N hydrogen bonds with lengths in the range 1.903-2.097 Å (see Table 2(d)). For this type of bonding there is only a small dependence on either the surface orientation or the surface site as reflected by the narrow range of variation in binding energies, i.e. 3.1 – 5.8 kcal/mol.

Beside the molecular adsorption of HCN species on the γ-Al_2O_3 surface we have further expanded our analysis to the case of dissociated species with the formation of adsorbed CN and H species. The main purpose of this analysis was to estimate the corresponding range of C-N vibrational frequencies for various configurations adsorbed on the surface. No attempt was made to map the potential energy surface for dissociation of HCN species on the γ-alumina surface leading to formation of either Al···CN or Al···NC species.

Specifically, CN species were considered to adsorb at unsaturated Al sites while the dissociated H atom binds to a surface O site, forming an OH group (see Figure 10). For CN radicals adsorption with C (see Figures 10(a), 10(d)), and N moieties (see Figures 10(b), 10(e)) oriented towards the surface were analyzed. As the dissociated H atoms can also interact with the adsorbed CN species in a manner which is dependent on the relative separations, a large number of configurations are possible. In our analysis here we limit ourselves to the case when the H atom is separated by the largest distance allowed by our slab model from the bonding site of C or N moieties. Beside the vertical configurations we have also identified states in which the dissociated CN species are lying down on the surface, with simultaneous bonding at both ends to Al surface sites. Such configurations are indicated in panels (c) and (f) of Figure 10 while corresponding results are given in Table 2(g).

On the based of the data given in Table 2(e) it can be seen that in the case of Al···CN bonding, the range of C-N vibrational frequencies is 2175 – 2188 cm^{-1} on the (100) surface, and 2179 – 2190 cm^{-1} on the (110) surface. Alternatively, in the case of Al···NC bonding, the C-N vibrational frequencies (see Table 2(f)) range from 2083 –

2087 cm^{-1} on the (100) surface while a range of 2079 – 2086 cm^{-1} was determined on the (110) surface (see Table 2(f)).

Finally, in the case of the lying down configurations Al···NC···Al, a significant frequency shift relative to gas phase values is observed, particularly in the case of the (110) surface. In this case the bonding to the surface involves the unsaturated Al_{III}(I) and Al_{IV}(II) sites (see Figure 10(f)). For this configuration we exemplify the effect of frequency shift when the H atom is moved away from the CN molecule. Specifically, in the case when the H atom is placed at a short distance (see Figure 10(f)), the CN vibrational frequency is 2118 cm^{-1}. By increasing the separation among H and CN species (see Figure 10g) the frequency is further shifted to higher values of 2150 cm^{-1} with a corresponding shortening of the CN bond from 1.176 Å to 1.169 Å

The ensemble of data presented in this section indicates a complex infrared spectral signature of HCN molecules when adsorbed on the γ-Al_2O_3 surface due to several factors. Among these we have analyzed here the influence of different bonding configurations such as molecular bonding at Al^{3+} Lewis acid sites or at Al-OH Brønsted acid sites, at Lewis base O sites with O···HCN hydrogen bond formation, or at mixed Al and O sites through an η^2(C, N) configuration. We noted important variations among the (100) and (110) surface orientations particularly due to the presence of different unsaturated Al sites. Furthermore, beside the molecular species, dissociated CN+H species can be also present on the surface. We have shown that orientations of CN species with either the C or N ends toward the surface, or simultaneous bonding at both C and N ends, as well as the presence of a dissociated H atom with OH formation at a nearby site, can lead to variations in the C-N vibrational frequencies. The complexity of

the experimental IR spectrum of HCN molecules on γ-Al_2O_3 is a reflection of superposition of all these contributions.

IV. Discussion

A. HCN Adsorption on Clean γ-Al_2O_3 Surfaces. Even though it has been observed that doped aluminum ions on oxide surfaces act as catalytic sites on the surface reaction of HCN molecules causing dissociation and polymerization,[3] there is a lack of studies of HCN adsorption on the γ-Al_2O_3 surface itself. Because of the different binding sites on γ-Al_2O_3 surfaces, several configurations for HCN molecular adsorption can occur: (a) $\boldsymbol{Al^{3+}}$···NCH (Lewis acid sites); (b) Al-O***H*** ···NCH (Brønsted acid sites); (c) Al-***O***-Al(or H)···HCN (Lewis base sites). These molecular adsorbed species have C-H (C-D) stretching vibrational modes shown in Figure 1 and 3. The isotope shift of C-H stretching mode by deuterium and ^{13}C labeling is -720 cm^{-1}, which is obtained from the difference of ν(C-H) mode frequency between **HC**N and **D**^{13}**C**N in the gas phase.[30] The vibrational modes at ~ 2604 cm^{-1} (sharp) and at 2600 cm^{-1} – 2300 cm^{-1} (broad) upon D^{13}CN exposure (see Figure 3) correlate with the modes at ~ 3300 cm^{-1} (sharp) and 3300 cm^{-1} – 2800 cm^{-1} (broad) upon HCN adsorption (see Figure 1) respectively, showing the same behavior. Frequency shifts in each case (sharp and broad) are observed to be about -700 cm^{-1}. Thus the abnormally broad band at 3300 cm^{-1} – 2800 cm^{-1} as well as the sharp peak at ~ 3300 cm^{-1} in HCN adsorption can be confirmed as ν(C-H) modes. The C≡N stretching modes in molecular adsorption are highly isotopically shifted in D^{13}CN from ~ 2097 cm^{-1} for HCN to ~ 1911 cm^{-1} for D^{13}CN (see Figure 4). This highly negative shift (-Δν = 191 – 197 cm^{-1}) is the result of a deuterium isotope effect as well. Only thermal depletion is

observed in these molecularly adsorbed species. It is shown that HCN binding to Lewis acid sites (***Al***$^{3+}$···NCH) is relatively strong compared to Brønsted acid sites (Al-O***H***···NCH) and Lewis base sites (Al-***O***-Al···HCN). The ν(C≡N) frequency of adsorbed HCN molecules at Brønsted acid sites (Al-O***H***···NCH) can not be separated from other species.

The existence of dissociative adsorption of HCN is proved by the separation of Al-CN (Al-NC) species from adsorbed HCN molecular species in the ν(^{13}C≡N) spectral region. Compared to the isotope shifts of D^{13}CN species (-Δν = 191 – 197 cm^{-1}), the isotope shifts of dissociated ^{13}CN species are smaller (-Δν = 40 – 50 cm^{-1}) for the ν(^{13}C≡N) mode. Since the Al-^{13}CN would be more affected by ^{13}C isotope labeling,[2] we can separate Al-^{13}CN from Al-N^{13}C species based on the isotopic shifts. Thus the prominent ^{13}C-labeled species at ~ 2060 cm^{-1} shifts to ~ 2100 cm^{-1} for ^{12}C-labeled species and is assigned to Al-N^{13}C; the ^{13}C-labeled species at ~ 2129 cm^{-1} shifts to ~ 2179 cm^{-1} for the ^{12}C-labeled species and is assigned to Al-^{13}CN, as shown Table 1. A -51 cm^{-1} isotope shift for Si-^{13}CN and a -39 cm^{-1} shift for Si-N^{13}C were observed by changing from ^{12}C to ^{13}C,[2] which is consistent with our results. These dissociation reactions accompany the development of isolated Al-OH (Al-OD) surface species, as seen in Figure 3.

Based on these assignments, these experimental results are correlated with the theoretical values as shown in Figure 11. The solid lines indicate the FWHM of the ν(C≡N) and ν(C=N) modes in each bonding configuration which is obtained from the curve-fitted FTIR spectra (Figure 2 and 5). The symbols are from the computed values in Table 2. In most cases excellent agreement is obtained. The theoretical frequency values

of ν(C≡N) in the Al-NC geometry deviate slightly from the experimental range. In addition, one of the Al-NC-Al configurations exhibits its theoretical ν(C≡N) frequency in the middle of the experimental range. Therefore the contribution of bridged forms of CN has been postulated. In the case of HCN adsorption on the highly unsaturated $Al_{III}(I)$ site on the (110) surface bound with the N end of the molecule, the theoretical vibrational frequency (~ 2201 cm^{-1}) occurs far away from the corresponding experimental observation. Since the $Al_{III}(I)$ site on the (110) surface is considered as the most reactive site on γ-Al_2O_3 surfaces, HCN molecules might not remain undissociated on this site.

However in the ν(C-H) region the highly red-shifted ν(C-H) frequency in the Al_2O···HCN configuration is also calculated to be in the range of 3150 cm^{-1} – 3200 cm^{-1} (compared to calculated ν(C-H) frequency, 3382 cm^{-1}, in gas phase) just as observed in the experiments. The ν(C-H) mode would be expected to be highly perturbed in this hydrogen-atom bound configuration.

Here, two possible mechanisms for the surface dissociative adsorption of HCN can be proposed. The first one requires that the C-H bond in Al^{3+}···N**C-H** species (on Lewis acid sites) is cleaved, and then the hydrogen atom is flipped to a nearby oxygen atom (Al-***O***-Al) to produce an Al-OH group. The second mechanism requires that the C-H bond of Al_2-O···**H-C**N species (on Lewis base sites) is broken producing the Al-OH group, followed by CN adsorption on an aluminum ion site. In both cases, the aluminum ion (Al^{3+}) sites are of importance. On a highly hydroxylated surface which is generated by the adsorption of large amounts of H_2O, where the aluminum ion sites are more fully coordinated, the Al-NC (Al-CN) as well as Al^{3+}···NCH species are not observed (data not

shown here). This shows that the aluminum ion (Al^{3+}) sites are the centers for the surface dissociative reaction of HCN.

A major finding in the present work is the observation of the η^2(C, N)-HCN bonding on the γ-Al_2O_3 surface. The η^2(C, N) configuration of nitrile groups on a surface, where both C and N atoms are simultaneously bonded to surface sites, was first proposed for acetonitrile adsorption on the Pt(111) surface.[31] Acetonitrile molecules form a saturated monolayer by η^2(C, N)-CH_3CN bonding. The ν(C≡N) frequency at ~ 2270 cm^{-1} observed in the multilayer disappears, and then a new feature at ~ 1615 cm^{-1} appears in ν(C=N) frequency region after annealing at 180 K. For the Al_2O_3 surface, the η^2(C, N)-CH_3CN adsorbed species is also observed by others at 1611 cm^{-1}.[32]

In the η^2(C, N)-HCN adsorbed configuration observed in this study, the CN stretching vibrational mode is also found at a much lower frequency (~ 1698 cm^{-1}, see Figure 5) than that of end-on adsorbed HCN species (~ 2200 – ~ 2000 cm^{-1}, see Figure 2). The ~ 1698 cm^{-1} mode is in the C=N double bonding region. The C≡N triple bond in the nitrile group converts to a C=N double bond by η^2 bonding. The observed ν(C=N) frequency in the η^2(C, N)-HCN species also matches the calculated values (1634 – 1710 cm^{-1}, see Table 2. b) and Figure 11). The thermal stability of η^2(C, N)-HCN species on the γ-Al_2O_3 surface is observed to be similar to the end-on adsorbed HCN on Lewis acid sites (Al^{3+}···NCH).

B. HCN Adsorption on TEDA-precovered γ-Al_2O_3 Surfaces. Because Brønsted acid sites and Lewis acid sites are occupied by pre-adsorbed TEDA (TEMA) on γ-Al_2O_3 surfaces,[12,33] most of the ν(C≡N) modes formed on clean Al_2O_3 surfaces are absent on TEDA(TEMA)-functionalized γ-Al_2O_3 surface as seen in Figure 6 and 7. Only

a minor spectral difference is found for HCN adsorption comparing TEDA- and TEMA-precovered surfaces in Figure 6 and 7. The small difference due to the different coverages of pre-adsorbed TEDA and TEMA as has been demonstrated in separate experiments (not shown here). The results of Figure 7 and Figure 8 indicate that no chemical interaction between adsorbed TEDA species and HCN occurs. The HCN species adsorbed on Lewis base sites (Al-***O***-Al) are also unaffected by TEDA.

In this work, it is shown that the presence of the exposed amine functionality of the adsorbed TEDA molecules for HCN adsorption is not important. Unlike silicate and charcoal supports, the alumina surface itself contains Al^{3+} ion sites where the HCN molecules are active. Therefore TEDA only competes with HCN for these sites on γ-Al_2O_3. The function of the TEDA molecules, employed with cations such as Cu^{2+}, Zn^{2+}, and Cr^{6+}, for HCN adsorption is to bind the cations by forming complexes with them. Such anchored cations then bind HCN. The effect of these anchored cations is therefore more important than TEDA molecules in causing HCN capture by the surface.

V. Summary

The adsorption of HCN on the γ-Al_2O_3 surface has been studied using transmission FTIR spectroscopy. It is demonstrated that the HCN molecule binds to Brønsted acid sites (Al-O***H***···NCH), Lewis acid sites (***Al***$^{3+}$···NCH), and Lewis base sites Al-***O***-Al(or H)···HCN on the γ-Al_2O_3 surface. In addition to molecular binding, HCN dissociative adsorption also occurs at 170 K, and it is enhanced by heating to 290 K. It is shown that aluminum ion (Al^{3+}) sites are centers for the surface dissociative reaction in which the H-CN bond is broken. In addition, η^2(C, N)-HCN bonding is also observed

with a ν(CN) frequency at ~ 1698 cm^{-1}, indicating the shift from a C≡N triple bond to a C=N double bond by the η^2 bonding of the nitrile group on γ-Al_2O_3.

No direct binding of HCN to the exposed amine group on TEDA pre-adsorbed on γ-Al_2O_3 is found. Instead the TEDA molecule effectively competes with HCN for binding sites on the γ-Al_2O_3 surface. The observed ν(C≡N) mode on a TEDA-precovered surface is due to the HCN adsorption on Lewis base sites (Al-***O***-Al) where TEDA does not bind.

VI. Acknowledgement

We acknowledge with thanks the support of this work by The Army Research Office, and discussion with Dr. Alex Balboa of Aberdeen Proving Ground. A grant of computer time at the Army Research Laboratory is also gratefully acknowledged.

References

(1) Low, M. J. D.; Ramasubramanian, N.; Ramamurthy, P.; Deo, A. V. *J. Phys. Chem.* **1968**, *72*, 2371.

(2) Morrow, B. A.; Cody, I. A. *J. Chem. Soc. Faraday Trans. I* **1975**, *71*, 1021.

(3) Kozirovski, Y.; Folman, M. *Trans. Faraday Soc.* **1964**, *60*, 1532.

(4) Raskó, J.; Bánsági, T.; Solymosi, F. *Phys. Chem. Chem. Phys.* **2002**, *4*, 3509.

(5) Szanyi, J.; Kwak, J. H.; Peden, C. H. F. *J. Phys. Chem. B.* **2005**, *109*, 1481.

(6) Ecob, C. M.; Clements, A. J.; Flaherty, P.; Griffiths, J. G.; Nacapricha, D.; Taylor, C. G. *The Science of the Total Environment* **1993**, *130/131*, 419.

(7) Mancuso, J.; McEachern, R. J. *Journal of Molecular Graphics and Modelling* **1997**, *15*, 82.

(8) Pickett, J. L.; Naderi, M.; Chinn, M. J.; Brown, D. R. *Separation Science and Technology* **2002**, *37*, 1079.

(9) Rossin, J. A.; Morrison, R. W. *Carbon* **1991**, *29*, 887.

(10) Naderi, M.; Pickett, J. L.; Chinn, M. J.; Brown, D. R. *J. Mater. Chem.* **2002**, *12*, 1086.

(11) Hurley, M. M.; Wright, J. B.; Balboa, A.; Lushington, G. H. *IEEE Proceedings of the 2003 User Group Conference* **2003**, 55.

(12) Kim, S.; Byl, O.; Yates, J. T., Jr. *J. Phys. Chem. B.* **2005**, *109*, 3499.

(13) Ballinger, T. H.; Wong, J. C. S.; Yates, J. T., Jr. *Langmuir* **1992**, *8*, 1676.

(14) Ballinger, T. H.; Yates, J. T., Jr. *Langmuir* **1991**, *7*, 3041.

(15) Peri, J. B.; Hannan, R. B. *J. Phys. Chem.* **1960**, *64*, 1526.

(16) Knözinger, H.; Ratnasamy, P. *Catal. Rev. Sci. Eng.* **1978**, *17*, 31.

(17) We thank Professor Roger Miller for supplying HCN for our work.

(18) Kim, S.; Sorescu, D.C.; Byl, O.; Yates, J. T., Jr., *J. Phys. Chem*. B **2006**, 110, 4742

(19) Kresse, G.; Hafner, J. *Phys. Rev.* **1993**, *B 48*, 13115.

(20) Kresse, G.; Furthmüller, J. *Comput. Mat. Sci.* **1996**, *6*, 15.

(21) Kresse, G.; Furthmüller, J. *Phys. Rev.* **1996**, *B 54*, 11169.

(22) Vanderbilt, D. *Phys. Rev.* **1990**, *B 41*, 7892.

(23) Kresse, G.; Hafner, J. *J. Phys. Cond. Matter* **1994**, *6*, 8245.

(24) Perdew, J. P.; Chevary, J. A.; Vosko, S. H.; Jackson, K. A.; Pedersen, M. R.; Singh, D. J.; Fiolhais, C. *Phys. Rev.* **1992**, *B 46*, 6671.

(25) Monkhorst, H. J.; Pack, J. D. *Phys. Rev.* **1976**, *B 13*, 5188.

(26) Digne, M.; Sautet, P.; Raybaud, P.; Euzen, P.; Toulhoat, H. *J. Catal.* **2004**, *226*, 54.

(27) Beaufils, J. P.; Barbaux, Y. *J. Chim. Phys.* **1981**, *78*, 347.

(28) Nortier, P.; Fourre, P.; Mohammed Saad, A. B.; Saur, O.; Lavalley, J. C. *Appl. Catal.* **1990**, *61*, 141.

(29) Peri, J. B. *J. Phys. Chem.* **1965**, *69*, 231.

(30) Pacansky, J.; Calder, G. V. *J. Phys. Chem.* **1972**, *76*, 454.

(31) Sexton, B. A.; Avery, N. R. *Surf. Sci*. **1983**, *129*, 21.

(32) Raskó, J.; Kiss, J. *Appl. Cat. A: General* **2006**, *298*, 115.

(33) Kim, S.; Byl, O.; Yates, J. T., Jr. *J. Phys. Chem. B.* **2005**, *109*, 6331.

TABLE 1: The Isotope Shifts of ν(C≡N) Modes and their Assignments (in units of cm^{-1})

HCN(g)	Isotopomer	Isotope shifts		Assignments		
2097[a]	1911[a] (D^{13}**CN**)(g)		-186	Gas Phase		
	2063[a] (H^{13}**CN**)(g)	-34				
HCN /Al_2O_3[b]	D^{13}**CN** /Al_2O_3[b]				**HCN** /TiO_2[c]	**HCN** /SiO_2[c]
2179	2129	-50		Al-CN (M-CN)[d]	2195	2213
2165						
2147	1956		-191	HCN on Lewis acid sites		
2110	2070	-40		Al-NC (M-NC)[d]	2147	2159
2100	2060	-40				
				(HCN on Brønsted acid sites)[d]	2096	2105
~ 2079	~1882		-197	HCN on Brønsted acid sites & Lewis base sites		

[a] The frequencies are from this work and ref. 30. [b] See the spectra in Figures 2 and 4.

[c, d] The frequencies in last column and their assignments in parentheses are from ref. 4.

TABLE 2: Calculated Equilibrium Distances, Adsorption Energies and Vibrational Frequencies for HCN, CN+H and NC+H Adsorbed on (100) and (110) Surfaces of the γ-Al_2O_3 Surface.[a]

System/ Surface	Site	d(Al…X)[b]	d(O...Y)/[c] d(H...N)	d(N-C)	d(C-H)	E_{ads}	ν(C-H)	ν(N-C)
a) Al...NCH Adsorption								
(100)	Al_V(II)	2.130		1.149	1.069	7.4	3398	2169
	Al_V(I)	2.166		1.150	1.070	8.0	3387	2155
	Al_V(III)	2.079		1.148	1.070	12.7	3393	2173
(110)	Al_{III}(I)	1.985		1.145	1.071	27.5	3386	2201
	Al_{IV}(II)	2.045		1.148	1.069	13.7	3402	2175
	Al_{IV}(III)	2.152		1.150	1.071	7.2	3385	2166
b) η^2(C,N)-HCN Adsorption								
(110)	Al_{III}(I), μ_3-O	1.880	1.469	1.250	1.091	17.6	3104	1634
	Al_{IV}(II), μ_2-O	1.881	1.451	1.250	1.093	11.8	3078	1652
	Al_{IV}(III),μ_3-O	1.839	1.443	1.424	1.097	9.6	3029	1710
c) O...HCN Adsorption								
(100)	μ_3-O		2.093	1.157	1.083	2.1	3193	2088
	μ_3-O		2.277	1.158	1.077	2.6	3285	2094
(110)	μ_2-O		1.968	1.158	1.086	5.3	3153	2084
	μ_3-O		1.995	1.157	1.084	2.2	3177	2090
d) OH...NCH Adsorption								
(100)	μ_1-Al_V(I)		2.097	1.154	1.070	3.1	3380	2124
	μ_1-Al_V(II)		1.970	1.154	1.070	5.0	3384	2126
	μ_1-Al_V(III)		1.916	1.154	1.070	4.9	3386	2128
(110)	μ_1-Al_{III}(I)		1.975	1.154	1.070	4.4	3383	2119
	μ_1-Al_{IV}(III)		1.903	1.154	1.070	5.8	3375	2127
	μ_2-Al_{IV}(III)		1.935	1.154	1.070	5.2	3383	2119
e) Al...CN + OH								
(100)	Al_V(II)	1.997		1.168				2175
	Al_V(I)	1.971		1.167				2188
	Al_v(III)	1.981		1.168				2173
(110)	Al_{III}(I)	1.952		1.166				2190
	Al_{IV}(II)	1.967		1.168				2179
	Al_{IV}(III)	1.965		1.167				2179

(Table 2 continued)

f) Al...NC + OH				
(100)	Al_V(II)	1.882	1.179	2087
	Al_V(I)	1.857	1.181	2084
	Al_v(III)	1.876	1.180	2083
(110)	Al_{III}(I)	1.831	1.181	2079
	Al_{IV}(III)	1.850	1.180	2086
g) Al..CN..Al + OH				
(100)	Al_V(III), Al_V(I)	2.088[d]	1.178	2077
		2.162		
(110)	Al_{III}(I), Al_{IV}(II)[e]	2.079	1.174	2118
		2.074		
	Al_{III}(I), Al_{IV}(II)[f]	2.005	1.169	2150
		2.046		

[a] Bond distances are given in Angstroms, adsorption energies in kcal/mol and vibrational frequencies in cm^{-1}. [b] X stands for N in the case of NCH or NC adsorption with the N atom towards the surface, and for C in the case of CN adsorption with the C atom towards the surface. [c] The bond distance d(O…Y) is considered in the case of NCH adsorption to a surface O atom through the N end, or to a C atom for NCH adsorption in a η_2 configuration, d(H…N) is considered in the case of OH…NCH adsorption. [d] For the Al..CN..Al configurations the first bond corresponds to the Al…N distance while the second to the Al…C distance. [e] Configuration with a H atom at a short separation (~ 2.1 Å) from NC. [f] Configuration with the H atom at a large separation (~ 3.7 Å) from NC.

Figure Captions

Figure 1. FTIR spectra for HCN adsorption on Al_2O_3 at 170 K followed by sequential heating to 290 K at an HCN equilibrium pressure of ~15 mTorr.

Figure 2. FTIR spectra for HCN adsorption on Al_2O_3 at 170 K followed by sequential heating to 290 K at an HCN equilibrium pressure of ~15 mTorr.

Figure 3. FTIR spectra for $D^{13}CN$ adsorption on Al_2O_3 at 170 K followed by sequential heating to 290 K at a $D^{13}CN$ equilibrium pressure of < 1 mTorr.

Figure 4. FTIR spectra for $D^{13}CN$ adsorption on Al_2O_3 at 170 K followed by sequential heating to 290 K at a $D^{13}CN$ equilibrium pressure of < 1 mTorr.

Figure 5. FTIR spectra for HCN adsorption on Al_2O_3 at 170 K upon raising the HCN equilibrium pressure.

Figure 6. FTIR spectra of the HCN adsorption on the TEDA-precovered Al_2O_3 surface at 170 K with increasing HCN exposure at P = ~ 1.0, ~5.0, and ~ 15 mTorr, compared to HCN adsorption on the clean Al_2O_3 surface at 15 mTorr (dashed line) from Figure 2. In order to remove the TEDA background in this region, the spectrum taken before admitting HCN (P(HCN) = 0) is subtracted from the spectra following HCN adsorption on the TEDA-precovered surfaces.

Figure 7. FTIR spectra for HCN adsorption on the TEDA, and TEMA-precovered Al_2O_3 surface at 170 K with an HCN equilibrium pressure of ~ 15 mTorr. The spectrum taken before admitting HCN (P(HCN) = 0) is subtracted from the spectra following HCN adsorption on the TEDA (TEMA)-precovered surfaces.

Figure 8. FTIR spectra of the TEDA/Al_2O_3 surface in the ν(C-H) and δ(C-N) frequency regions upon HCN adsorption, showing the lack of an HCN effect on the spectra of adsorbed TEDA.

Figure 9. Representative configurations of the HCN molecule adsorbed on (100) (panels a)-c)) and (110) (panels d)-g)) γ-Al_2O_3 surfaces. Possible bonding configurations of the HCN molecule as Al…NCH (panels a) and d)), O…HCN (panels b) and f) or OH…NCH (panels c) and g)) are illustrated. In the case of the (110) surface, panel e) illustrates the η^2(C,N)-HCN bonding type.

Figure 10. Representative configurations of the CN radical adsorbed on (100) (panels a) - c)) and (110) (panels d)- f)) γ-Al_2O_3 surfaces. Bonding through the C end (panels a) and d)), the N end (panels b) and e)) or through a bridge configuration (panels c), f) and g)) are illustrated. Panels f) and g) illustrate the case when the dissociated H atom binds at two different surface O sites near (~2.1 Å), and further away (~3.7 Å) from the CN species. In the case of panels c), f) and g) the slab orientation is rotated 90° relative to the other panels in order to allow a clearer view of the bridge CN species.

Figure 11. Correlation between experimental and computed vibrational frequencies of HCN and CN species adsorbed on Al_2O_3 surfaces. Solid lines indicate FWHM of the ν(C≡N) and ν(C=N) band in each binding configuration which are measured from the curve-fitted FTIR spectra (Figure 2 and 5). Triangle symbols are from the computational results given in Table 2. The theoretical values were divided by a correction factor, 1.004768 = 2107 cm^{-1} /2097 cm^{-1} (= ratio between theoretical and experimental ν(C≡N) frequency values for gas phase HCN).

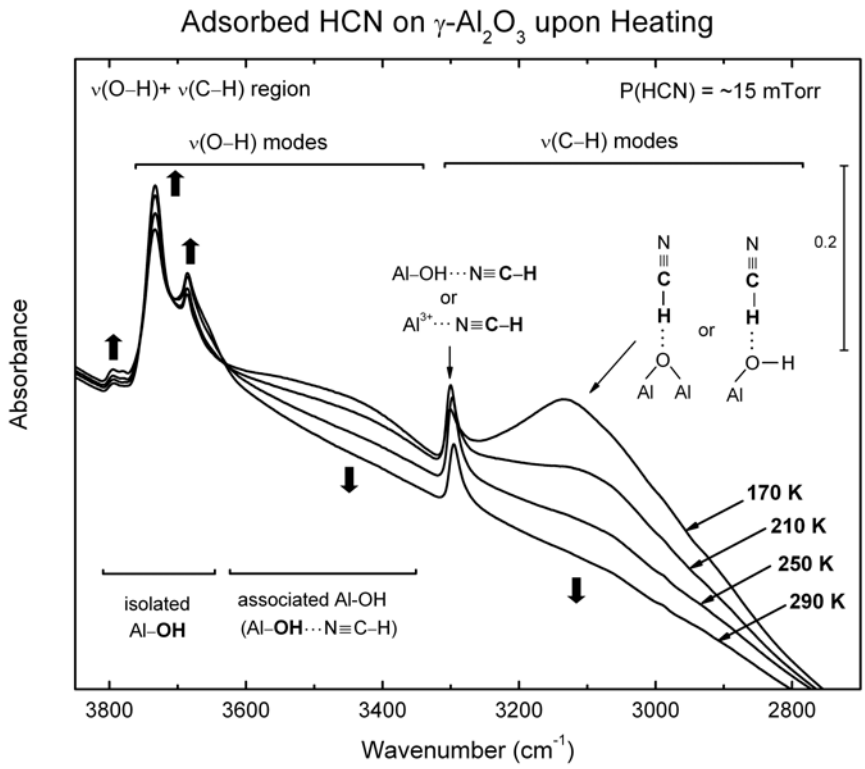

Fig 1. S. Kim et al.

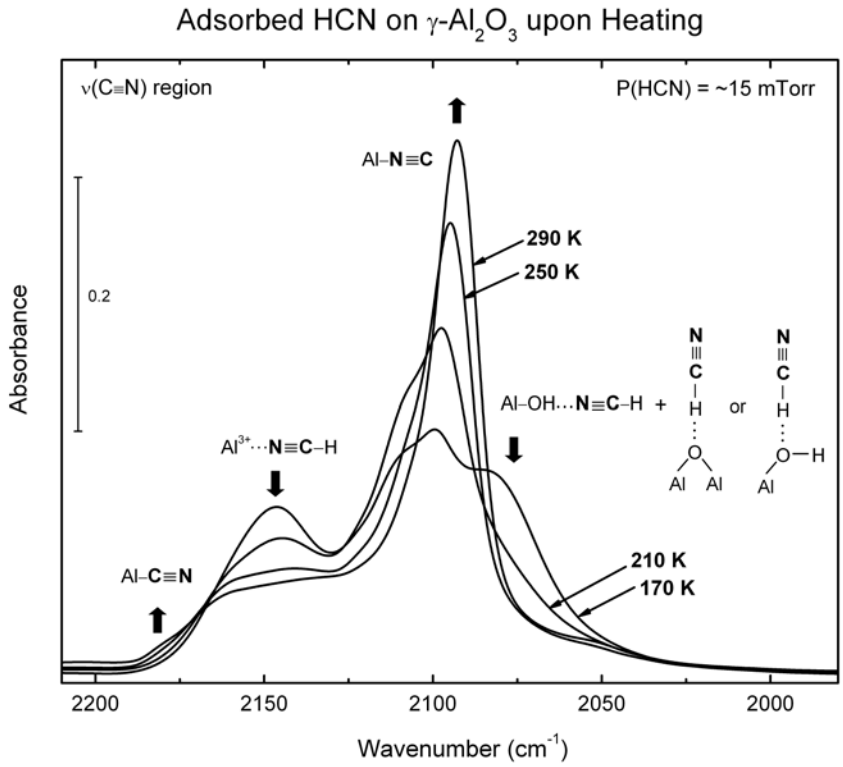

Fig 2. S. Kim et al.

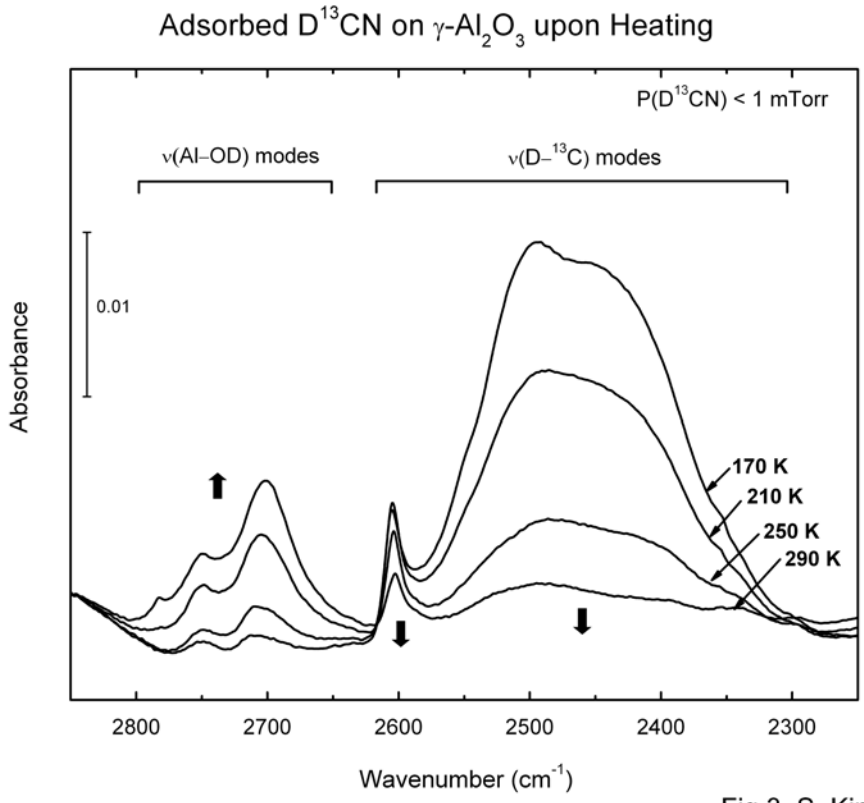

Fig 3. S. Kim et al.

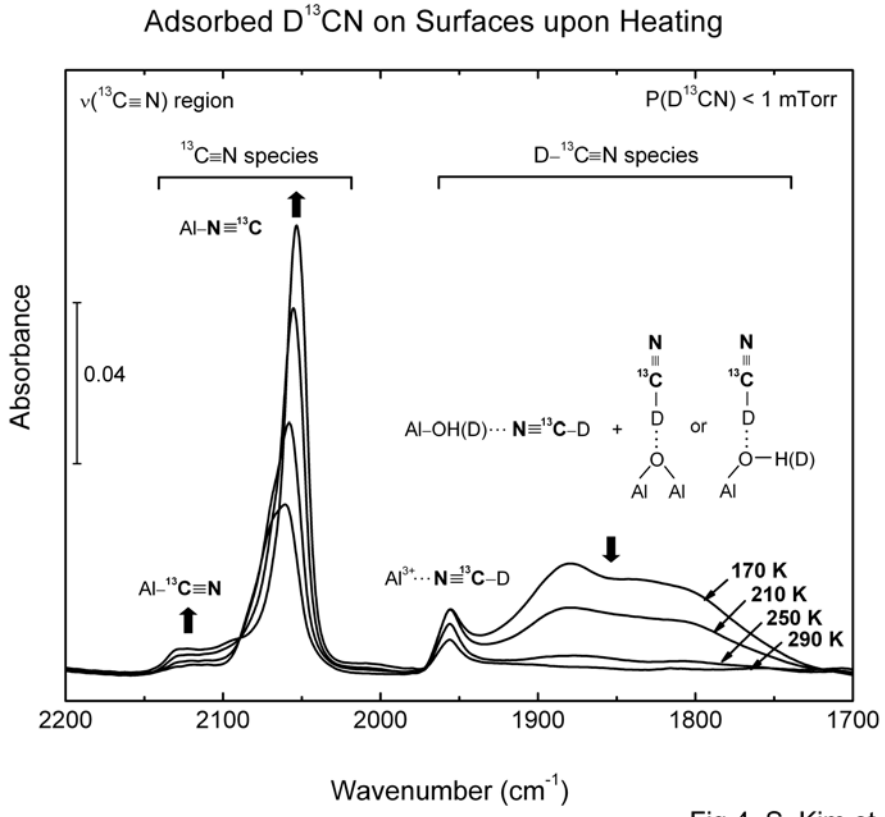

Fig 4. S. Kim et al.

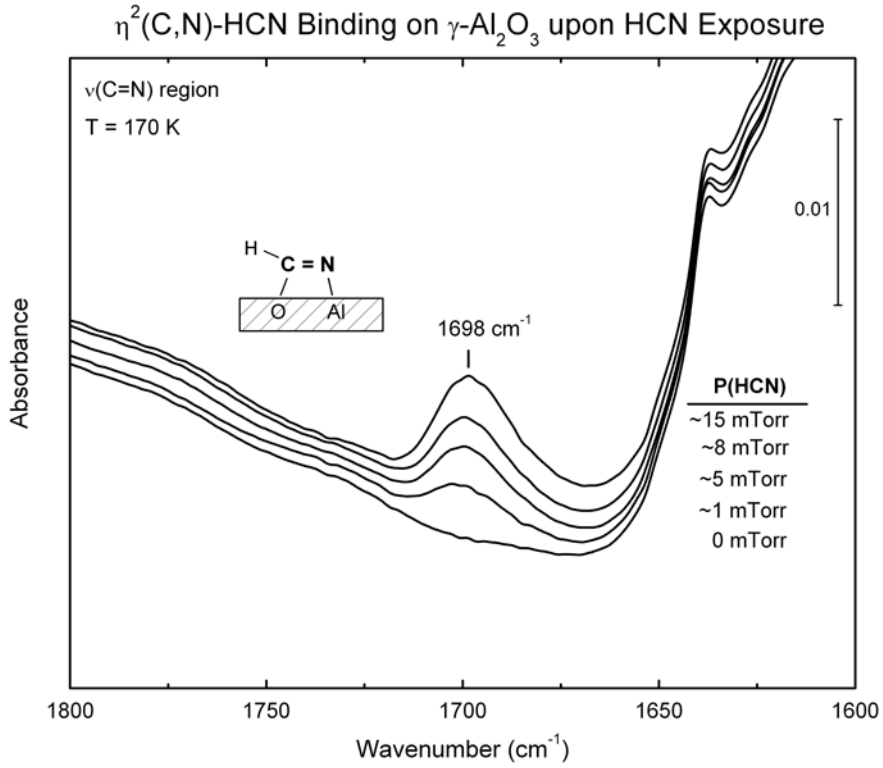

Fig 5. S. Kim et al.

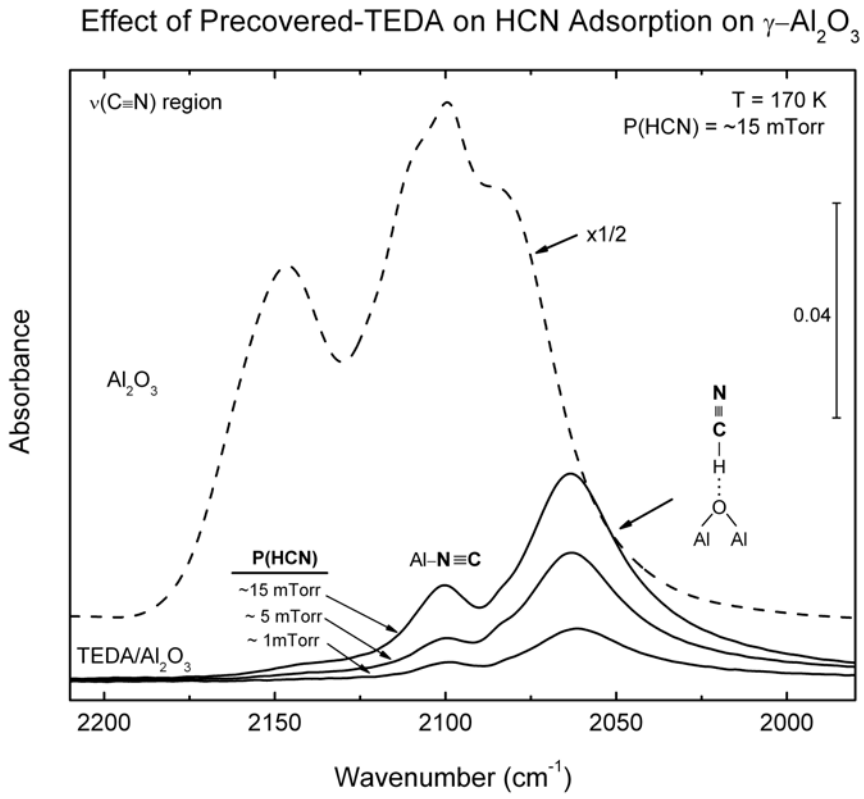

Fig 6. S. Kim et al.

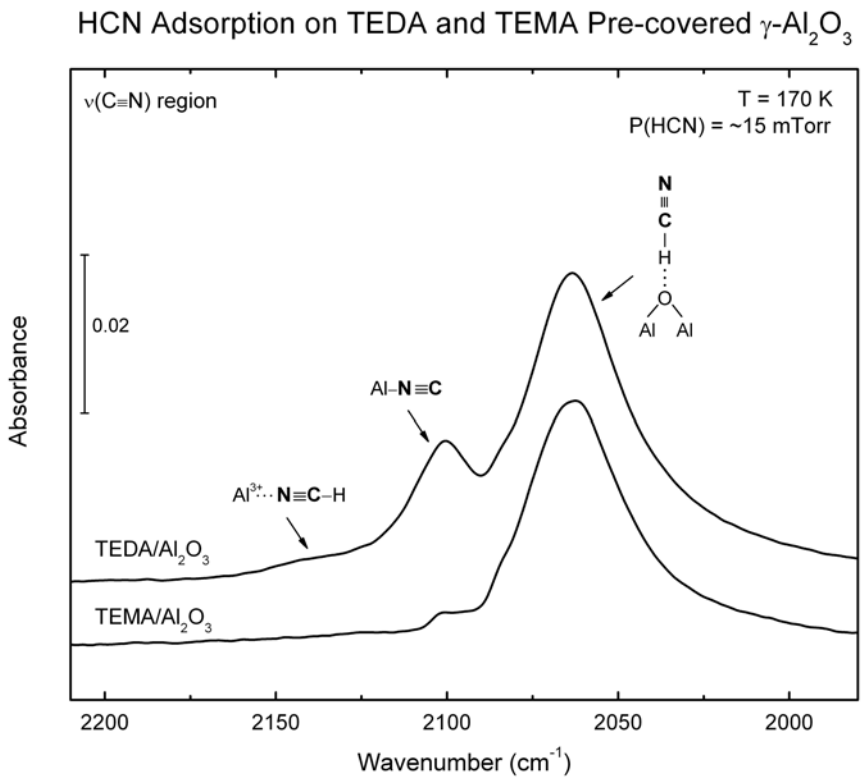

Fig 7. S. Kim et al.

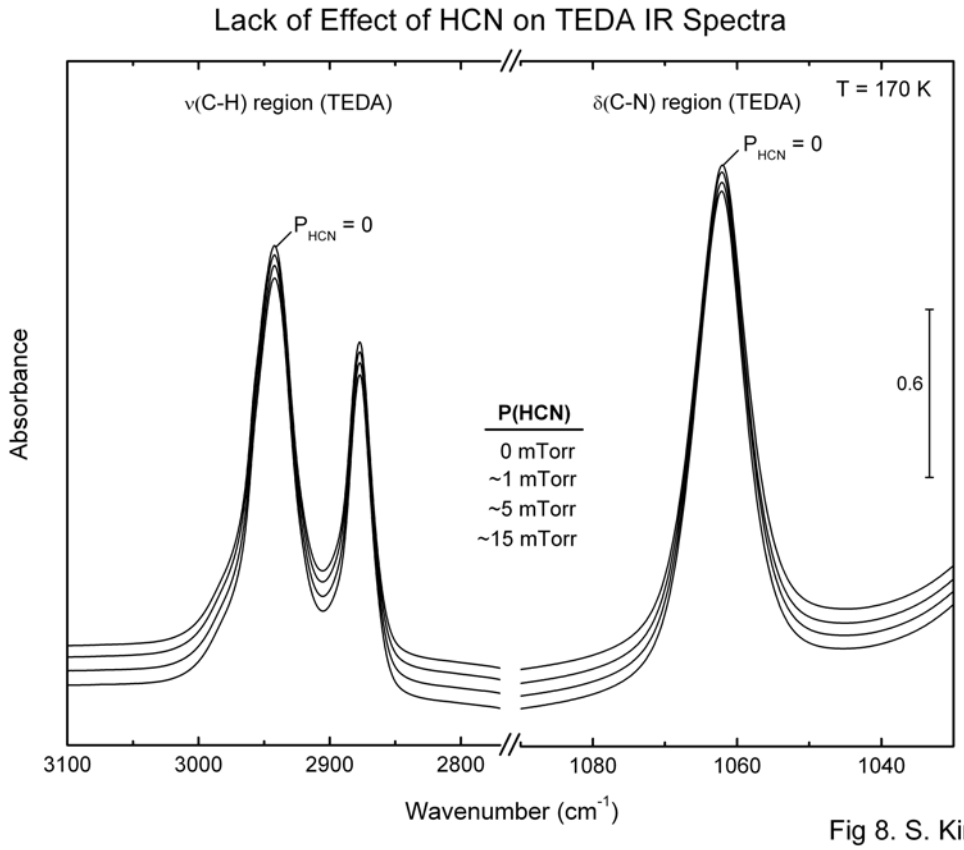

Fig 8. S. Kim et al.

Calculated Structures for HCN Interaction with γ-Al_2O_3

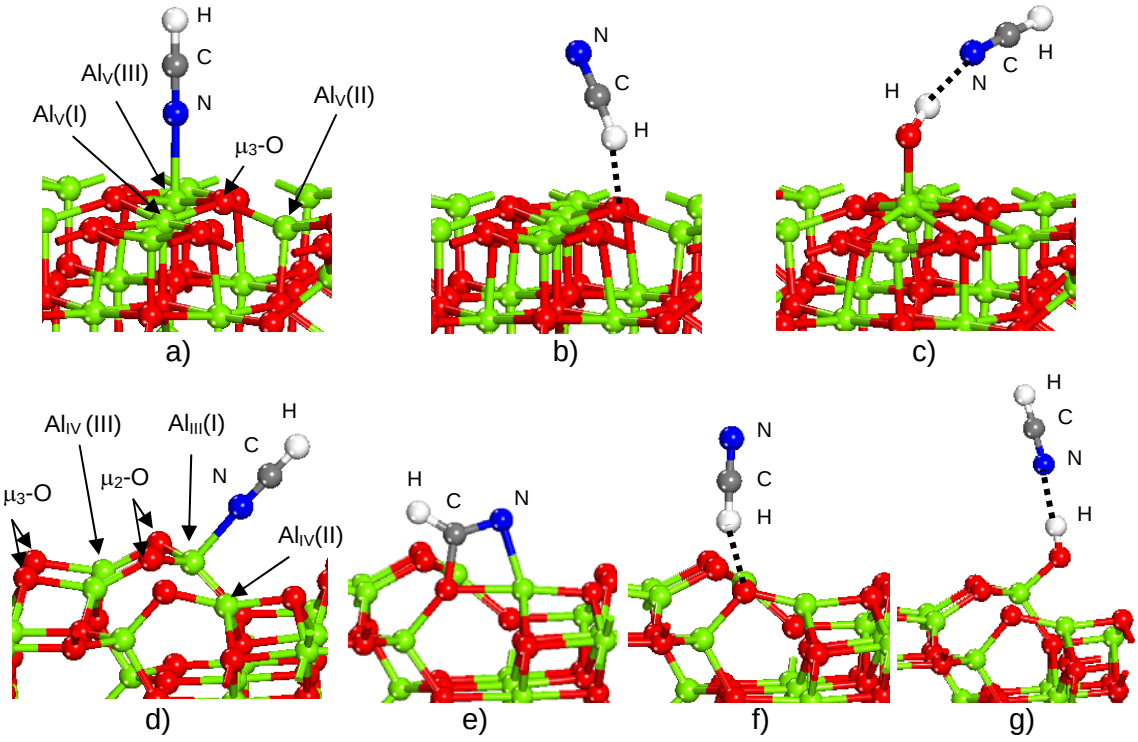

Fig 9. S. Kim et al.

Calculated Structures for CN Species on γ-Al_2O_3

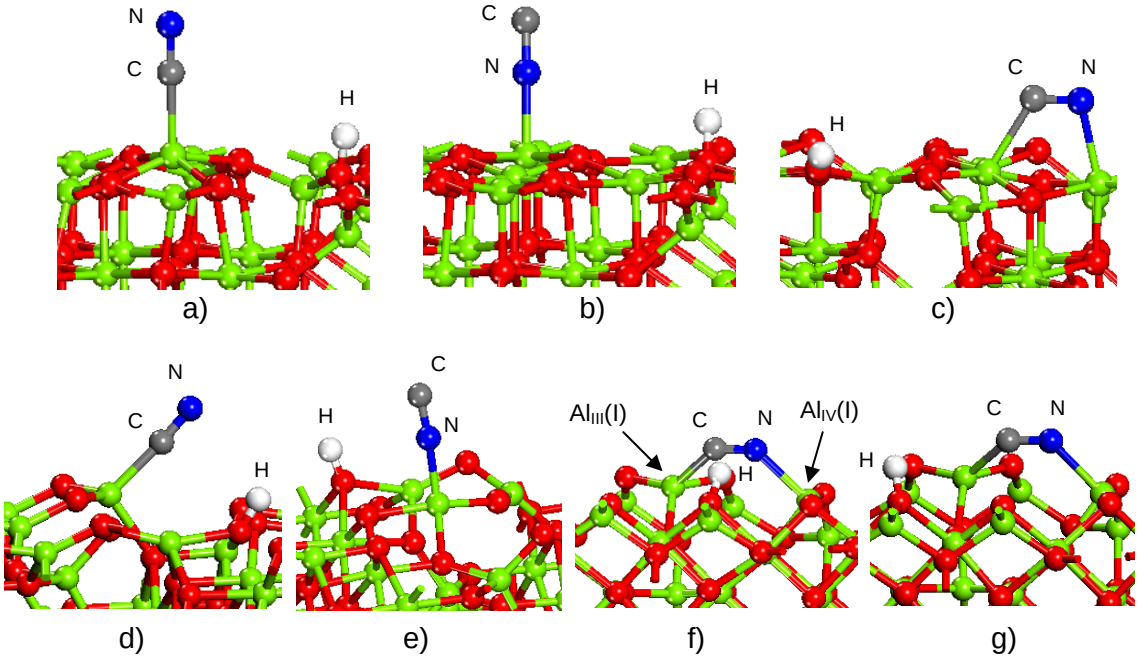

Fig 10. S. Kim et al.

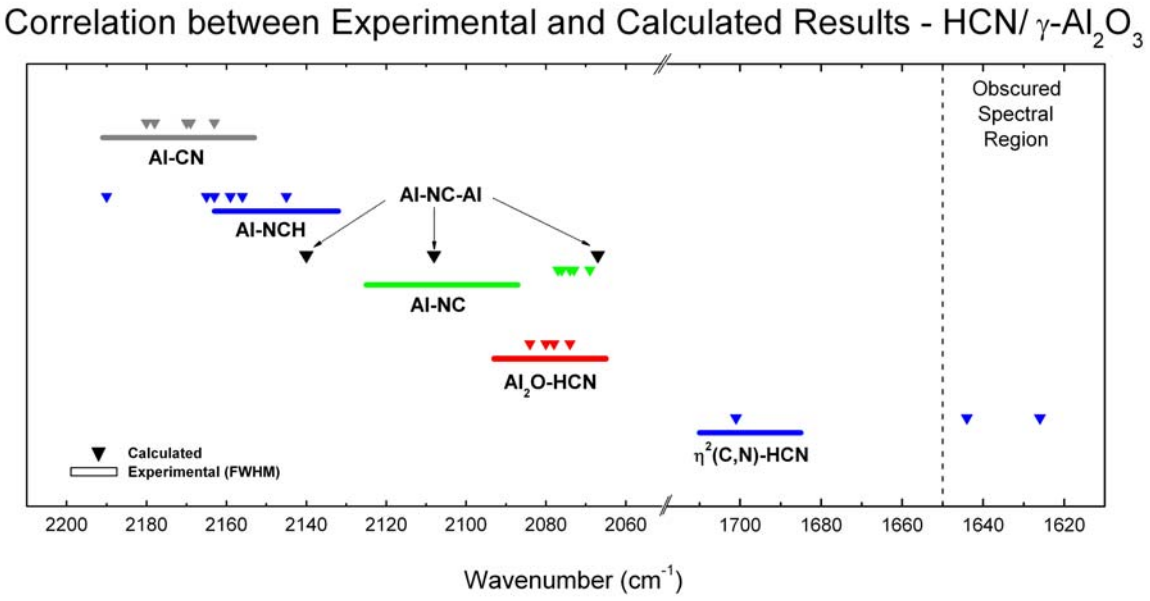

Fig 11. S. Kim et al.